ANL-6932

Argonne National Laboratory

DATA RELATING TO THE PRODUCTION OF TRANSCURIUM ELEMENTS IN HIGH NEUTRON FLUXES

by

D. C. Stewart, R. W. Anderson,
and John Milsted

LEGAL NOTICE

Printed in USA. Price $2.00. Available from the Clearinghouse for Federal Scientific and Technical Information, National Bureau of Standards, U. S. Department of Commerce, Springfield, Virginia

ANL-6932
Physics
(TID-4500, 34th Ed.)
AEC Research and
Development Report

ARGONNE NATIONAL LABORATORY
9700 South Cass Avenue
Argonne, Illinois 60440

DATA RELATING TO THE PRODUCTION OF TRANSCURIUM ELEMENTS IN HIGH NEUTRON FLUXES

by

D. C. Stewart, R. W. Anderson,
and John Milsted

Chemistry Division

September 1964

Operated by The University of Chicago
under
Contract W-31-109-eng-38
with the
U. S. Atomic Energy Commission

TABLE OF CONTENTS

DATA RELATING TO THE PRODUCTION OF TRANSCURIUM ELEMENTS IN HIGH NEUTRON FLUXES

by

D. C. Stewart, R. W. Anderson,
and John Milsted

INTRODUCTION

Milsted, Fields, and Metta[1] have published calculated yield curves showing the formation rates and levels of production of the very heavy nuclides when certain transneptunium isotopes are exposed for varying lengths of time in a series of high neutron fluxes. Since publication these authors have modified certain of the cross sections and half-lives they had originally assumed, partly on the basis of newly published information,[2] and partly because of adjustments made to bring the calculated isotopic compositions of the various product elements more in line with compositions observed experimentally in a series of research samples processed over the last decade. Using these new data, Milsted, Fields and Metta have now repeated their earlier calculations.[3]

In the present work, the computer programs used in calculating these new yield curves have been extended and modified to obtain additional data of interest to those individuals concerned with the practical questions of encapsulating, irradiating, and processing the target materials. Among these questions are:

(1) Will enough helium be formed by alpha decay of the target and its products during the irradiation to produce dangerous pressures in the irradiation can or target rod under reactor conditions?
(2) What will the maximum heat release be from the target at various flux levels, i.e., what will the target-cooling problem be?
(3) What will be the handling problem with respect to neutron emission from spontaneously fissioning nuclides at the time the sample is removed from the reactor?
(4) What will the problem of alpha containment be?
(5) What will the problem of β-γ shielding be?

Data are given in the form of curves relevant to the first four of these questions. The problem of β-γ hazard is a much more difficult one to solve, but it is hoped that it can be made the subject of a later separate report. Approximate curves are included here, however, to indicate the rate at which the various targets are converted to fission products at different flux levels as a rough indication of the magnitude of the gamma problem

For convenience, the buildup path assumed for the yield curves is reproduced in Figure 1. The basic and derived data used in the calculations are summarized in Tables 1 and 2, and the results of the calculations are given in Figures 2 through 24. The simple calculation methods used to obtain the required factors for application to the yield curves are given in Appendix A.

Table 1

DECAY AND CROSS-SECTION DATA

Nuclide	Half-lives		Natural Decay (Per μg)			Cross Sections			Helium Buildup
				Spontaneous Fission		Capture		Fission (b)	
	Nonspontaneous Fission	Spontaneous Fission	dis/sec (Nonspontaneous Fission)	fissions/sec	neutrons/sec	b	cm^2/g		cc/day/g
Pu^{238}	89.6 y	3.8×10^{10} y	6.22×10^{5}	0.0015	0.0054	403	1.03	16.8	0.002
Pu^{239}	24360 y	5.5×10^{15} y	2270	1×10^{-8}	3.4×10^{-8}	340	0.86	810	7.2×10^{-6}
Pu^{240}	6580 y	1.22×10^{11} y	8380	4.51×10^{-4}	0.0017	530	1.34	0	2.7×10^{-5}
Pu^{241}	13 y		4.23×10^{6}			350	0.88	1100	
Pu^{242}	3.79×10^{5} y	7.1×10^{10} y	144	7.7×10^{-4}	0.0029	50	0.125	0	4.6×10^{-7}
Pu^{243}	4.98 h		9.57×10^{10}			170	0.42	130	
Pu^{244}	$\sim 7.6 \times 10^{7}$ y	2.5×10^{10} y	~0.72	0.0022	0.0082	1.5	0.004	0	2.3×10^{-9}
Pu^{245}	11 h		4.3×10^{10}					260	
Am^{241}	458 y	2.3×10^{14} y	1.20×10^{5}	2.4×10^{-7}	9×10^{-7}	50 (to Am^{242m}) 620 (to Am^{242})	0.13 1.56	3.1	3.8×10^{-4}
Am^{242m}	152 y		3.59×10^{5}			5500	13.8	6400	
Am^{242}	16.0 h		2.99×10^{10}					3000	
Am^{243}	7600 y		7150			150	0.37	0	2.3×10^{-5}
Am^{244}	26 m		1.1×10^{12}					2000	
Cm^{242}	162.5 d	7.2×10^{6} y	1.23×10^{8}	7.6	29	30	0.075	0	0.39
Cm^{243}	35 y		1.56×10^{6}			250	0.62	590	0.005
Cm^{244}	17.9 y	1.346×10^{7} y	3.03×10^{6}	4.01	15.2	35	0.086	0	0.0097
Cm^{245}	14000 y		3850			300	0.74	1850	1.2×10^{-5}
Cm^{246}	6600 y	1.66×10^{7} y	8170	3.23	12.3	7	0.017	0	2.6×10^{-5}
Cm^{247}	$>4 \times 10^{7}$ y		<1.34			50	0.12	200	4.3×10^{-9}
Cm^{248}	4.7×10^{5} y	4.6×10^{6} y	113	11.6	44	8	0.020	0	3.2×10^{-7}
Cm^{249}	64 m		4.4×10^{11}						
Bk^{249}	310 d	6×10^{8} y	6.26×10^{7}	0.088	0.34	800	1.95	0	
Bk^{250}	3.20 h		1.45×10^{11}			350	0.85	650	
Cf^{249}	360 y	4.5×10^{8} y	1.48×10^{5}	0.2	0.45	270	0.66	1600	4.7×10^{-4}
Cf^{250}	13.2 y	16600 y	4.00×10^{6}	3180	12100	1330	3.22	0	0.013
Cf^{251}	~ 800 y		~66000			2000	4.83	3000	2.1×10^{-4}
Cf^{252}	2.64 y	85.5 y	1.97×10^{7}	6.13×10^{5}	2.33×10^{6}	9	0.022	0	0.061
Cf^{253}	19 d		1.0×10^{9}			2	0.005	0	
Cf^{254}	-	60.5 d		3.14×10^{8}	1.19×10^{9}	2	0.005	0	
Cf^{255}	7 d		2.7×10^{9}					500	
Es^{253}	20.03 d	6.3×10^{5} y	9.55×10^{8}	83	315	200 to 37 h 7 to 480 d	0.48 0.017		3.1
Es^{254}	480 d	1.5×10^{5} y	3.96×10^{7}	346	1310	40	0.095	2000	0.13
Es^{254}	37 h	$>10^{5}$ y	1.23×10^{10}	<520	<1980				
Es^{255}	24 d		7.9×10^{8}			40	0.095	0	
Fm^{254}	3.38 h	246 d	1.35×10^{11}	7.73×10^{7}	2.94×10^{8}	100	0.24		430
Fm^{255}	21.5 h	1.2×10^{4} y	2.12×10^{10}	4300	16400	100	0.24	100	68
Fm^{256}	-	3 h	-	1.5×10^{11}	5.7×10^{11}	20	0.047	0	
Fm^{257}	100 d		1.9×10^{8}			100	0.24	100	0.6
Fm^{258}	-	5 h		9×10^{10}	3.4×10^{11}	5	0.012	0	
Fm^{259}	10 d		1.9×10^{9}			100	0.23	50	
Md^{259}	3.5 d		5.3×10^{9}			250	0.58	0	17
Md^{260}	10 h		4.5×10^{10}					1050	

Table 2

FISSION AND HEAT DATA

Nuclide	Induced Fission f/sec/μg at Flux of:			Heat, W/μg				
				From Induced Fission at Flux of:			From Spontaneous Fission	From Nonspontaneous Fission
	2×10^{15}	5×10^{15}	1×10^{16}	2×10^{15}	5×10^{15}	1×10^{16}		
Pu^{238}	8.5×10^{7}	2.1×10^{8}	4.2×10^{8}	0.0028	0.007	0.014	5×10^{-14}	5.6×10^{-7}
Pu^{239}	4.1×10^{9}	1.0×10^{10}	2.0×10^{10}	0.14	0.35	0.70	3×10^{-19}	1.9×10^{-9}
Pu^{240}							1.5×10^{-14}	7.0×10^{-9}
Pu^{241}	5.5×10^{9}	1.4×10^{10}	2.8×10^{10}	0.18	0.45	0.90		1.4×10^{-8}
Pu^{242}							3×10^{-14}	1.2×10^{-10}
Pu^{243}	6.5×10^{8}	1.6×10^{9}	3.2×10^{9}	0.022	0.055	0.11		0.0089
Pu^{244}							7×10^{-14}	5.2×10^{-13}
Pu^{245}	1.3×10^{9}	3.2×10^{9}	6.4×10^{9}	0.043	0.11	0.22		0.0083
Am^{241}	1.6×10^{7}	3.9×10^{7}	7.8×10^{7}	5×10^{-4}	1.3×10^{-3}	2.6×10^{-3}	8×10^{-17}	1.1×10^{-7}
Am^{242m}	3.2×10^{10}	7.8×10^{10}	15.6×10^{10}	1.07	2.63	5.33		3.5×10^{-8}
Am^{242}	1.5×10^{10}	3.7×10^{10}	7.4×10^{10}	0.50	1.25	2.5		0.0028
Am^{243}								6.2×10^{-9}
Am^{244}	9.9×10^{9}	2.5×10^{10}	5.0×10^{10}	0.33	0.80	1.65		0.26
Cm^{242}							2.5×10^{-10}	1.2×10^{-4}
Cm^{243}	2.9×10^{9}	7.2×10^{9}	1.4×10^{10}	0.097	0.24	0.48		1.5×10^{-6}
Cm^{244}							1.3×10^{-10}	2.9×10^{-6}
Cm^{245}	9.1×10^{9}	2.3×10^{10}	4.6×10^{10}	0.31	0.78	1.55		3.5×10^{-9}
Cm^{246}							1.1×10^{-10}	7.1×10^{-9}
Cm^{247}	9.8×10^{8}	2.4×10^{9}	4.8×10^{9}	0.033	0.08	0.16		$>1.1 \times 10^{-12}$
Cm^{248}							3.9×10^{-10}	8.3×10^{-11}
Cm^{249}								0.062
Bk^{249}							3×10^{-12}	1.1×10^{-6}
Bk^{250}	3.2×10^{9}	8×10^{9}	1.6×10^{10}	0.10	0.25	0.50		0.044
Cf^{249}	7.8×10^{9}	2.3×10^{10}	4.6×10^{10}	0.26	0.65	1.30	4×10^{-12}	1.5×10^{-7}
Cf^{250}							1.1×10^{-7}	3.9×10^{-6}
Cf^{251}	1.45×10^{10}	3.6×10^{10}	7.3×10^{10}	0.48	1.20	2.40		6.5×10^{-8}
Cf^{252}							2.1×10^{-5}	1.9×10^{-5}
Cf^{253}								4.3×10^{-5}
Cf^{254}							0.011	-
Cf^{255}	2.4×10^{9}	6.0×10^{9}	1.2×10^{10}	0.08	0.20	0.40		4.3×10^{-4}
Es^{253}								0.001
Es^{254}	9.5×10^{9}	2.4×10^{10}	4.8×10^{10}	0.32	0.80	1.60		4.1×10^{-5}
Es^{254} (37 h)								0.0022
Es^{255}								4.8×10^{-5}
Fm^{254}							0.0026	0.16
Fm^{255}	4.7×10^{8}	1.2×10^{9}	2.4×10^{9}	0.016	0.04	0.08	1.4×10^{-7}	0.024
Fm^{256}							5	-
Fm^{257}	4.7×10^{8}	1.2×10^{9}	2.4×10^{9}	0.016	0.04	0.08		1.4×10^{-4}
Fm^{258}							3	-
Fm^{259}	2.3×10^{8}	5.7×10^{8}	1.2×10^{9}	0.008	0.02	0.04		3×10^{-4}
Md^{259}								0.006
Md^{260}	4.9×10^{9}	1.2×10^{10}	2.5×10^{10}	0.16	0.40	0.80		0.007

SCOPE OF WORK

At the present time, production of macro amounts of the "synthetic" elements above uranium can be accomplished only by adding neutrons to the U^{238} nucleus in a high-flux reactor (this picture may possibly soon be modified by the use of "instant" reactors, i.e., controlled underground nuclear explosions). As weighable amounts of each of the heavier elements derived from uranium have become available over the last twenty years, they have been separated, purified, and repackaged for reactor exposure to serve as base material in turn for the production of elements of still higher mass. Intermediate nuclides used in this cycling process were originally formed either as the primary products of certain reactor operations (as was Pu^{239}), or as byproducts from such operations (as in the cases of Am^{241} and Np^{237}). The cycling process with such intermediate materials (primarily with Pu^{239}) has brought about the present stage of development in which multigram quantities of nuclides of mass of 242 or higher are now, or soon will be, available to serve as target materials for the next step in the cyclic process.

Because of the vagaries of fission and capture cross sections, decay half-lives, etc., certain nuclides of each element have longer survival times during the buildup process and thus tend to dominate the isotopic composition of that element during much of the irradiation period. Nuclides of this type are Pu^{242}, Am^{243}, Cm^{244}, and Cf^{252}. These four will be considered in the present work as the most probable candidates over the next few years as targets for still heavier element production. Three neutron-irradiation flux levels were chosen for the calculations, based on the characteristics of two very high-flux reactors soon to be available or in the planning stage: the Oak Ridge High Flux Isotope Reactor (HFIR) and the Argonne Advanced Research Reactor (A^2R^2). Fluxes chosen were 2×10^{15} $n/cm^2/sec$ (estimated to be the average flux in the HFIR center thimble), 5×10^{15} $n/cm^2/sec$ (HFIR maximum flux, A^2R^2 average center thimble flux) and 1×10^{16} $n/cm^2/sec$ (A^2R^2 maximum flux).

Two possible target nuclides, Am^{241} and Np^{237}, which could be made available in very large amounts as byproducts from production reactor operations, were not considered in the present study. Since the buildup path based on Np^{237} goes through Pu^{239}, the latter isotope itself is the more reasonable target, being available in quantity.

The nuclide Am^{241} is a more subtle case. The first step in its buildup path involves the formation of two nuclear isomers of Am^{242}, both of which have very high fission cross sections.(4) In moderately high fluxes, a usable amount of buildup can occur past the Am^{242} stage, but in very high fluxes the destruction rate at this point in the chain is so large as to make the material of little use as a raw material for production of heavier elements.

Am^{241} does, however, have much utility as a starting nuclide for forming large quantities of Cm^{242}, an isotope that is of considerable interest because of its intense alpha activity and its promise as a compact energy source. A separate report is being prepared on that subject.[5]

METHOD OF CALCULATION

The calculations were carried out with an IBM 1620 (II) computer, programmed by means of the FORTRAN (II) coding system. The basic growth and decay program was that of Milsted, Fields and Metta,[3] which uses the analytic solution of differential equations originally due to Bateman.[6] However, this solution breaks down if any two members of the chain have identical destruction constants, as in the case of a chain involving feedback through alpha decay to a nuclide already included in the chain. In these cases, the integration process was carried out numerically, by considering the formation and destruction of each member of the chain during successive small time intervals. In order to achieve accuracy comparable with that of the Bateman solution, it was necessary to make these time increments quite small (10^4 sec in most cases), and each calculation therefore involved many thousands of iterations to cover irradiation times up to several years. The calculations were therefore considerably slower than when using the Bateman solution.

The input and output cards for either program were identical in format. The input cards specified the half-lives and cross sections for formation and destruction of each nuclide, and the irradiation times required. The output cards gave relative yields (atoms of product per initial target atom) at each specified irradiation time. The output from either program could be used as data for the final calculations.

The alpha and neutron activities, and the heat output were calculated by applying the appropriate conversion factors from Tables 1 and 2 to the relative yield data, summing, and normalizing to one gram of starting material.

The rate of helium production at any time could be calculated from the sum of the alpha activities of the important alpha emitters and from the helium-production factor. The accumulation of helium during the interval between two successive time values was approximated from the rate of production at the mean relative yields and the length of the time interval. These helium increments were then summed to give the cumulative data shown in the curves.

The data for total fission product accumulation were calculated by adding the relative yields of all transuranium nuclides present and subtracting from unity. The result of this calculation is strictly the total

relative yield of the products of all competing reactions resulting in loss of atoms from the buildup chains. However, since all-important neutron-capture processes were included in the buildup chains, the calculation gave a good approximation to the relative number of target atoms undergoing fission. The use of these yield figures as mass fission product percentages ignores any gain in mass by neutron capture before fission and the mass of the fission neutrons lost. For the present purpose, however, these inaccuracies were considered unimportant.

DATA USED (Tables 1 and 2)

The basic data presented in Tables 1 and 2 are the decay half-life and cross-section values, the other numbers being derived from them as indicated in Appendix A. For the most part, the basic values were taken from reference (3), supplemented where needed by information from the compilations of Isaac and Wilkins[7] of Hyde[8], and from the Isotope Tables prepared by Strominger, Hollander, and Seaborg.[9]

It should be realized that many of the quoted cross sections and half-lives (particularly for the transcalifornium isotopes) are still very poorly known; in some cases, the values in the tables are simply estimates based on systematics or experimental yield considerations.

THE BUILDUP PATH (Figure 1)

Figure 1 presents the buildup path assumed in the present study. In the case of the Pu^{242}, Am^{243}, and Cm^{244} targets, the contribution of "feedback" (i.e., the cycling back into the buildup chain of daughter nuclides formed by natural decay during the irradiation period) can be ignored. In the case of the Cf^{252} target, however, the relatively short half-life of the parent target (leading to rapid Cm^{248} daughter production) combined with the relatively low destruction cross section of Cf^{252} does cause an appreciable contribution which must be considered. (This is particularly true for the calculations of heat production from Cf^{252} targets, owing to the presence of highly fissionable Cf^{251} in the feedback chain.) This particular reverse cycle is accordingly indicated in Figure 1. Feedback paths from the alpha decays of Fm^{254} and Es^{253} (yielding Cf^{250} and Bk^{249}, respectively) were also included in the calculations for Cf^{252}. Although these paths contributed appreciably to the heat production, they are omitted from Figure 1 for the sake of clarity.

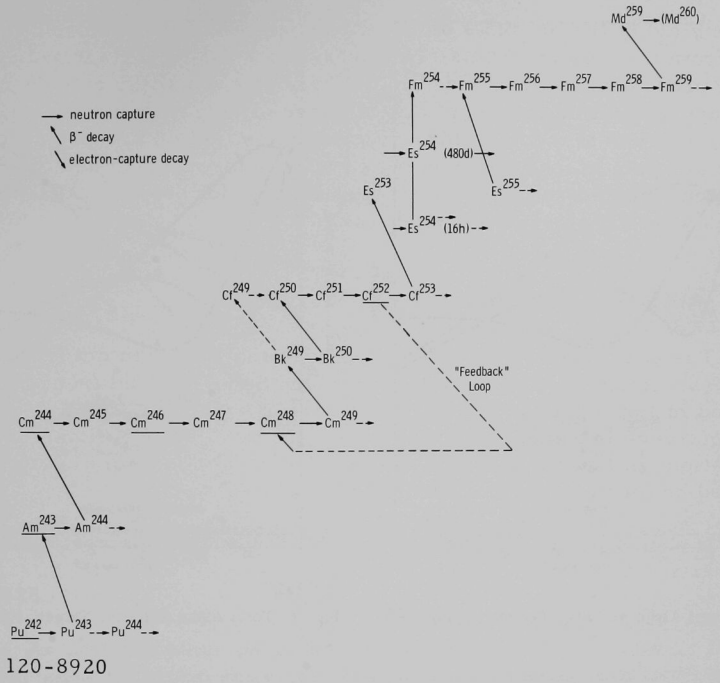

Fig. 1. Assumed Buildup Path

ALPHA EMISSION (see Figures 2-6)

Of the four target materials studied, three (Pu^{242}, Am^{243}, and Cm^{244}) showed quite similar patterns for all of the properties calculated. This fact can be really understood when it is realized that there are only two mass units separating their initial weights, and that the three form a very compact chain with short-lived intermediates ($Pu^{242} \longrightarrow Pu^{243} \xrightarrow{5\ hr} Am^{243} \longrightarrow Am^{244} \xrightarrow{26\ min} Cm^{244}$). Thus the patterns of the various curves at a given flux tend to be separated only in time, as can be seen in the "C" curves of Figures 2-3-4. With a Pu^{242} target, the first large alpha-emission peak (due to Cm^{244}) occurs after about 6 weeks at a flux of 1×10^{16} $n/cm^2/sec$; with Am^{243}, the peak appears in about 2 weeks; with Cm^{244}, of course, it is at zero time. In all three cases, a sharp drop in alpha activity occurs as the Cm^{244} is burned out, but a second smaller peak then appears as Cf^{252}, Es^{253}, and Fm^{254} grow in. This is shown in Figure 5, which presents a detailed picture of the contribution of the various products to alpha emission when Cm^{244} is irradiated at a flux of 5×10^{15} $n/cm^2/sec$.

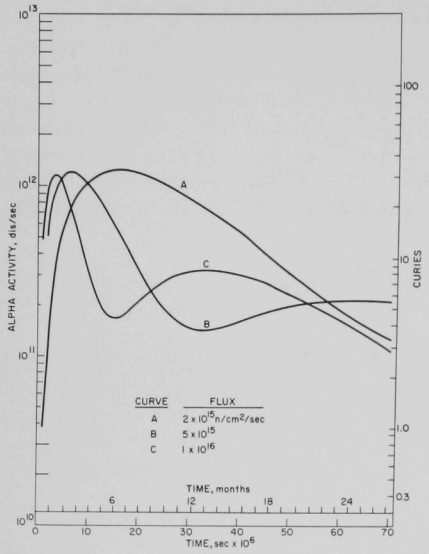

120-8921

Fig. 2. Total Alpha Activity. Target: 1 gram Pu^{242}.

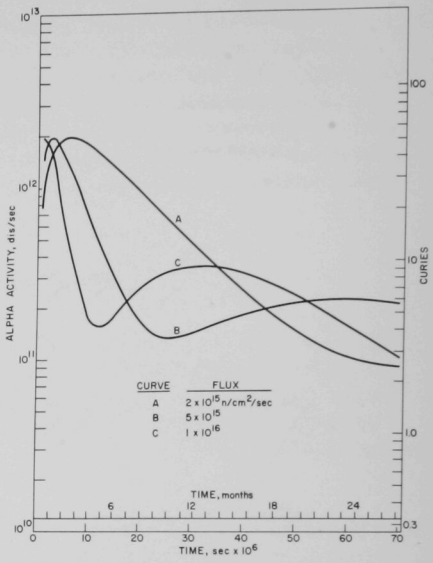

120-8922

Fig. 3. Total Alpha Activity. Target: 1 gram Am^{243}.

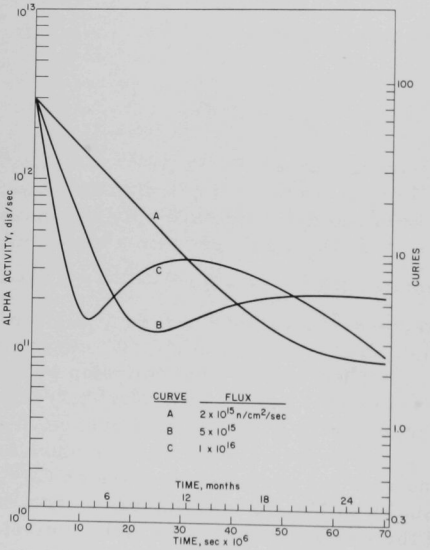

120-8923

Fig. 4. Total Alpha Activity. Target: 1 gram Cm^{244}.

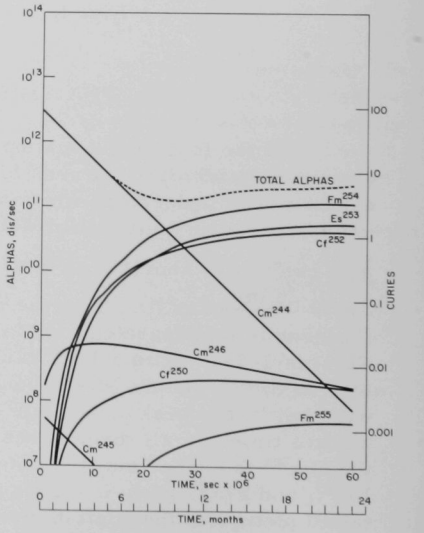

120-8924

Fig. 5. Detail - Alpha Emission. 1 gram Cm^{244} at 5 x 10^{15} Flux.

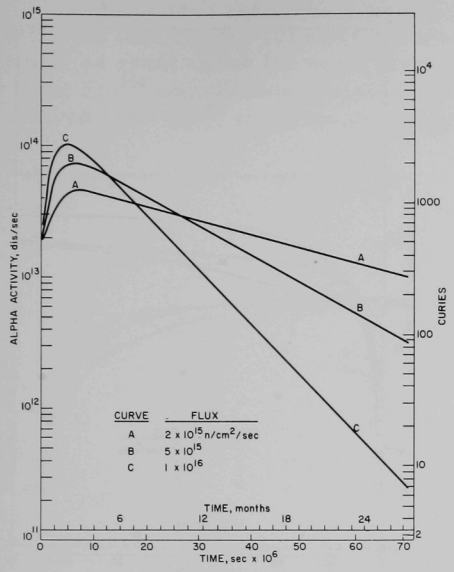

120-8925

Fig. 6

Total Alpha Activity.
Target: 1 gram Cf^{252}.

As with the other parameters calculated, the Cf^{252} case is somewhat atypical when its alpha-emission curves are compared with those of the other three targets. Total alpha-emission levels higher by some factors of ten are reached than in the case of the lighter targets, with the emission curves at all three fluxes showing a single peak some one or two months after the start of the irradiation. This peak arises primarily from the contribution of the 3.38-hr Fm^{254}. In practice, this short half-life means that a substantial decrease in the alpha activity of the sample would ordinarily occur between the time of removal from the reactor and the beginning of processing. On the other hand, the Fm^{254} contribution to the helium-accumulation problem (see next section) will be very large.

HELIUM ACCUMULATION (see Figures 7-10)

As would be expected from the alpha-emission curves, the helium-accumulation data for the Pu^{242}, Am^{243}, and Cm^{244} targets are very similar to each other, all leveling off at between 1- and 2-ml total helium buildup per gram of target (see Figures 7-9). There is an interesting reversal in the curves for long irradiations in that less total helium is formed at the higher fluxes, simply indicating that at these very high fluxes the very intense alpha emitters have a shorter residence time in the reactor before they are transmuted or fissioned.

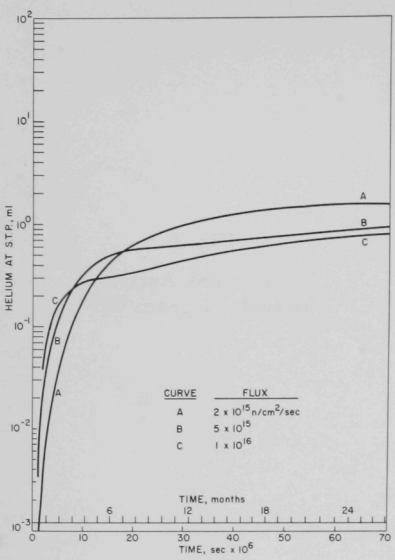

120-8926

Fig. 7. Cumulative Helium from α Activity. Target: 1 gram Pu^{242}.

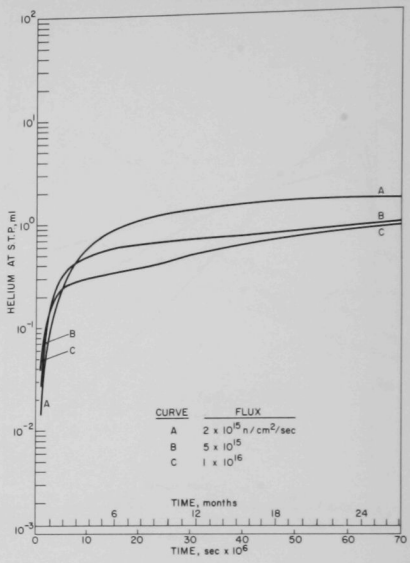

120-8927

Fig. 8. Cumulative Helium from α Activity. Target: 1 gram Am^{243}.

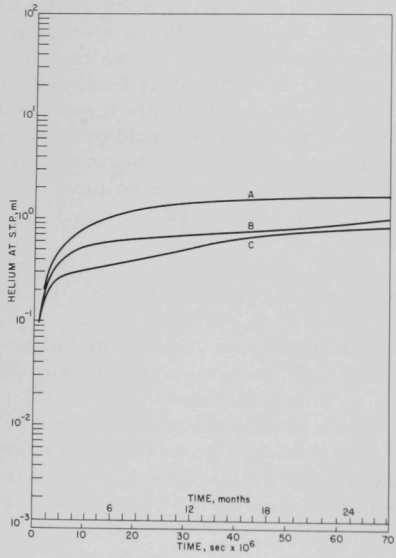

120-8928

Fig. 9

Cumulative Helium from α Activity. Target: 1 gram Cm^{244}.

As pointed out in the previous section, the Cf^{252} case is decidedly different (see Figure 10) since the total alpha accumulation is some fifty times as great as for the other targets during long irradiations. In addition to the Fm^{254} contribution discussed above, substantial quantities are also derived from Es^{253} and from the original Cf^{252} target itself.

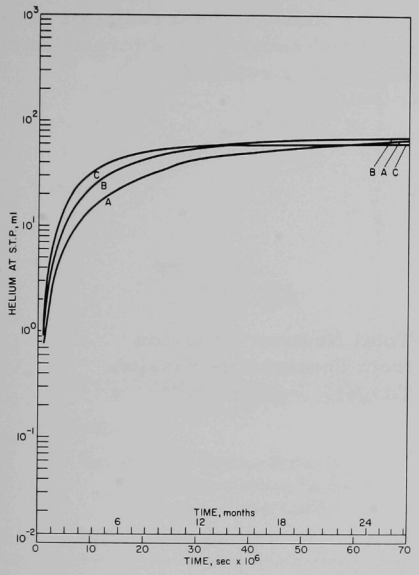

120-8929

Fig. 10

Cumulative Helium from α Activity.
Target: 1 gram Cf^{252}.

NEUTRON EMISSION (see Figures 11-15)

In the case of all four target nuclides, the neutron emission from spontaneous fission is essentially determined by the level of Cf^{252} and Cf^{254} production. This is best demonstrated in Figure 14, which indicates the contribution made by individual products to the total neutron output per gram of sample when Cm^{244} is irradiated in a flux of 5×10^{15} n/cm^2/sec. As with earlier parameters, the three lighter targets show very similar curves of neutron growth (see Figures 11-13) and all eventually reach essentially the same emission level.

With a Cf^{252} target (see Figure 15), a dramatic increase occurs in the total neutron output in the 1×10^{16}-n/cm^2/sec flux comparatively early in the irradiation, although the growth over the initial emission level is very slight at 2×10^{15} n/cm^2/sec, but substantial at 5×10^{15} n/cm^2/sec. These peaks (all occurring in the range of 4 to 6 months of irradiation time) are due to formation and eventual destruction of 60.5-d Cf^{254}, which is

believed to decay essentially completely by spontaneous fission. Heavy-element-production programs based on the use of Cf^{252} in very high fluxes are required to be very cognizant of the Cf^{254} problem in designing shielding for facilities for processing the irradiated targets. However, since most of the buildup products of interest reach their maximum concentrations in a Cf^{252} target in slightly less than two months (see Figure 16 of Reference 3), the Cf^{254} hazard can be partially mitigated by planning the irradiation program around a shorter processing schedule and removing the target from the reactor before the maximum emission point is reached.

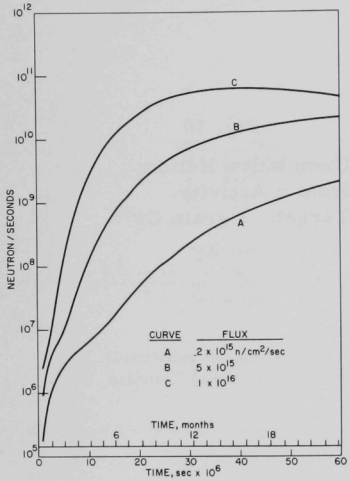

120-8930

Fig. 11

Total Neutron Emission
from Spontaneous Fission.
Target: 1 gram Pu^{242}.

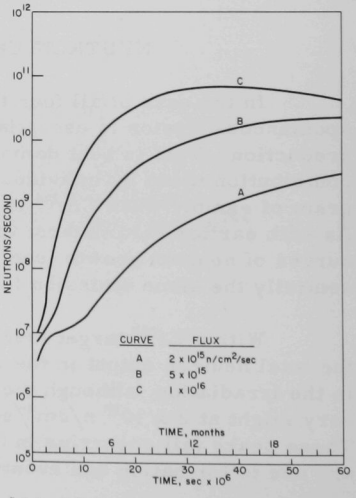

120-8931

Fig. 12

Total Neutron Emission
from Spontaneous Fission.
Target: 1 gram Am^{243}.

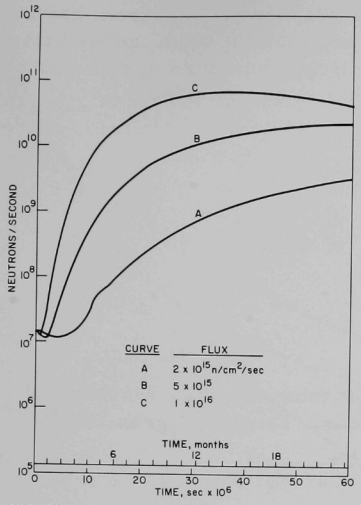

120-8932

Fig. 13. Total Neutron Emission from Spontaneous Fission. Target: 1 gram Cm^{244}.

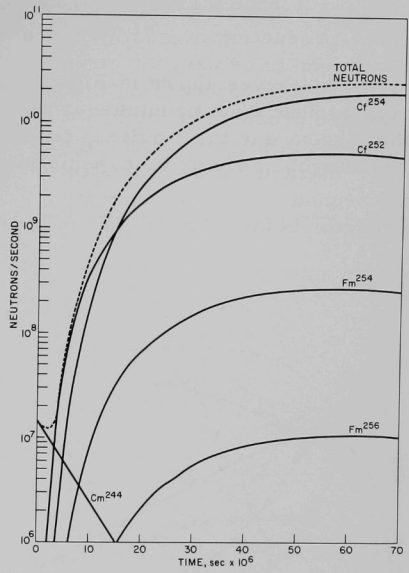

120-8933

Fig. 14. Detail - Neutrons from Spontaneous Fission. 1 gram Cm^{244} in 5 x 10^{15} Flux.

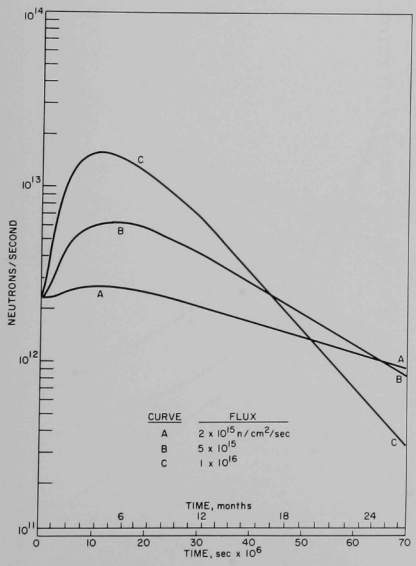

120-8934

Fig. 15

Total Neutron Emission from Spontaneous Fission. Target: 1 gram Cf^{252}.

HEAT FROM ACTINIDE FISSION AND DECAY
(see Figures 16-20)

The curves shown in Figures 16-20 include (a) heat from natural decay, (b) heat from spontaneous fission, and (c) heat from induced fission in the targets and their buildup products. Heat of capture of pile neutrons on the fission products or capsule materials is not included.

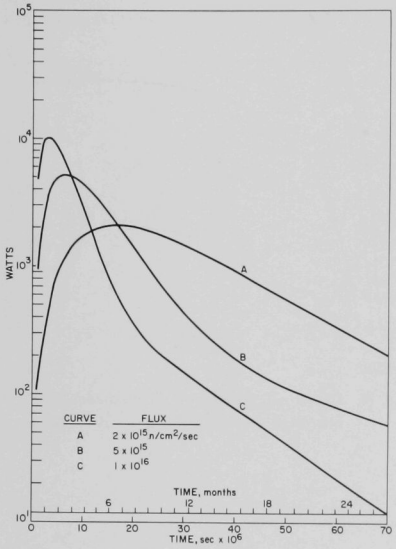

120-8935

Fig. 16

Heat from Actinide Fission and Decay. Target: 1 gram Pu^{242}.

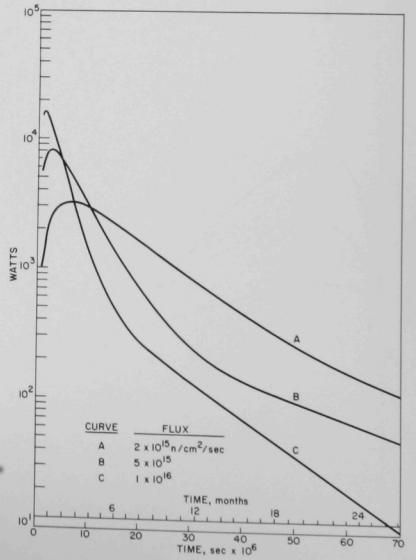

120-8936

Fig. 17

Heat from Actinide Fission and Decay. Target: 1 gram Am^{243}.

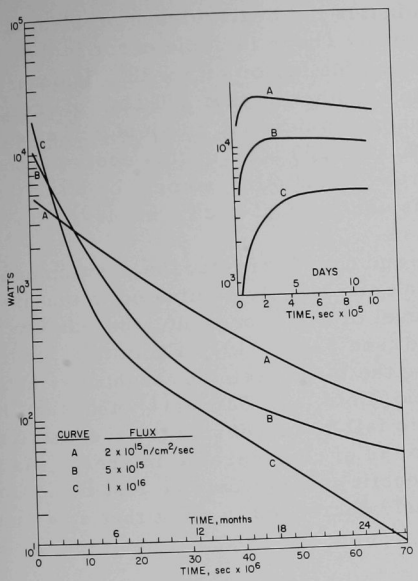

120-8937

Fig. 18. Heat from Actinide Fission and Decay. Target: 1 gram Cm^{244}.

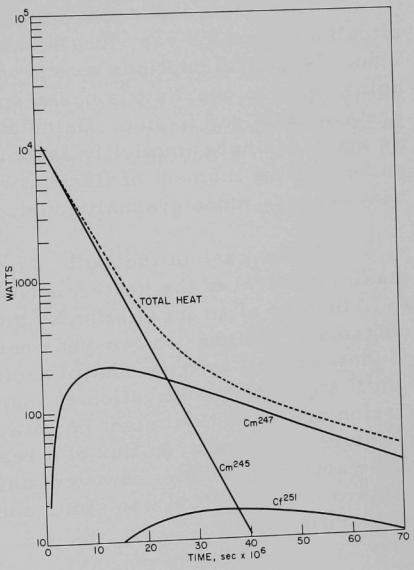

120-8938

Fig. 19. Detail - Heat from Fission and Decay. 1 gram Cm^{244} in 5 x 10^{15} Flux.

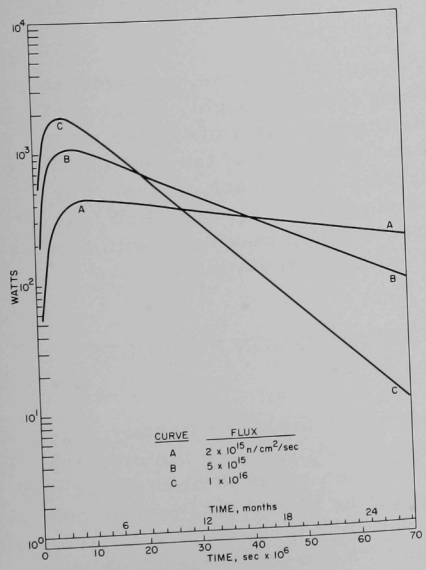

120-8939

Fig. 20

Heat from Fission and Decay.
Target: 1 gram Cf^{252}.

Heat from induced fission dominates the heat-release problem in all situations save for very long irradiations. There is some error in the induced-heat calculations as shown, since the factor of 3×10^{10} fissions/sec being equal to one Watt is based on the assumption that 200 MeV of energy are available per fission. Calculations based directly on yield curves such as are made here implicitly assume that all 200 MeV of this energy appear as heat at the moment of fission, whereas in actuality some 7 or 8% of the heat appears more gradually during fission product decay, etc.(10)

In the case of the Pu^{242}, Am^{243}, and Cm^{244} targets, the position and maximum level of the heat-release peak are largely dominated in the first 8-12 months of an irradiation by the level of Cm^{245} present, whereas Cm^{247} controls in the one- to two-year period (see Figure 19). From this point of view as well as from that of avoiding the large actinide target loss in the Cm^{245} stage, the observation of Diamond, Coté, and Barnes(11) that the Cm^{245} fission cross section might be caused to fall by increasing the thermal temperature of the neutron flux of a reactor is of considerable interest. (As these authors indicate, however, any benefit gained would be lost if the Cm^{245} capture cross section was simultaneously decreased, a point that still must be clarified.)

As can be seen from the insert graph on Figure 18, the point of maximum heat release with the Cm^{244} target appears in the very early stages of an irradiation. In a flux of 1×10^{16} n/cm^2/sec the peak is reached in less than 2 d at the very respectable level of better than 18,000 W/g of target material.

Cf^{252} is a comparatively lesser problem from the heat-release point of view, the maximum value attained being less by roughly a factor of ten (see Figure 20) than those seen for starting materials of lighter mass. As indicated in an earlier section, a substantial amount of the heat that is released in this case comes from Cf^{251} arising in feedback cycles. For example, in a flux of 1×10^{16} n/cm^2/sec a maximum value of 340 W/g is obtained if feedback is ignored, whereas the corresponding maximum with feedback is 1880 W/g (both peaks being at $5\text{-}6 \times 10^6$ sec irradiation).

RATE OF TARGET CONVERSION TO FISSION PRODUCTS
(see Figures 21-24)

The similarities in the rates with which the three lighter targets are destroyed is again apparent from Figures 21-23, in which the primary differences in the families of curves for each element is their displacement to the left in going from Pu^{242} to Cm^{244}, reflecting primarily the time necessary to reach the Cm^{245} stage in each case. The Cf^{252} target, for which the buildup chain does not involve a step comparable with the Cm^{245} roadblock in the lighter elements, has a comparatively long lifetime in the reactor (see Figure 21).

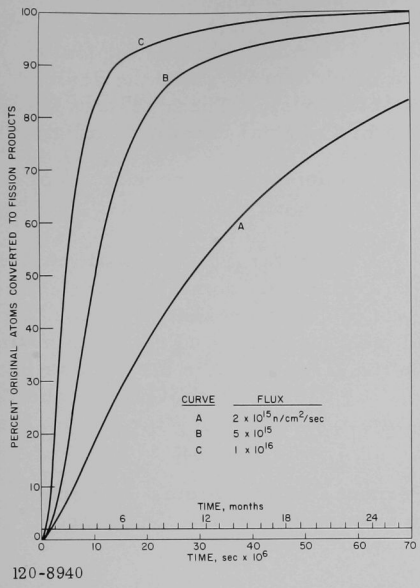

120-8940

Fig. 21. Percent Original Atoms Converted to Fission Products. Pu^{242} Target.

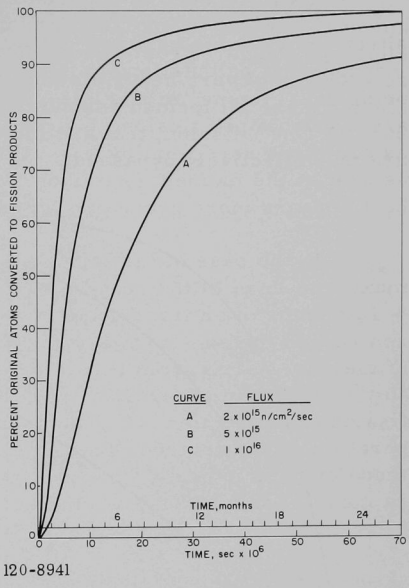

120-8941

Fig. 22. Percent Original Atoms Converted to Fission Products. Am^{243} Target.

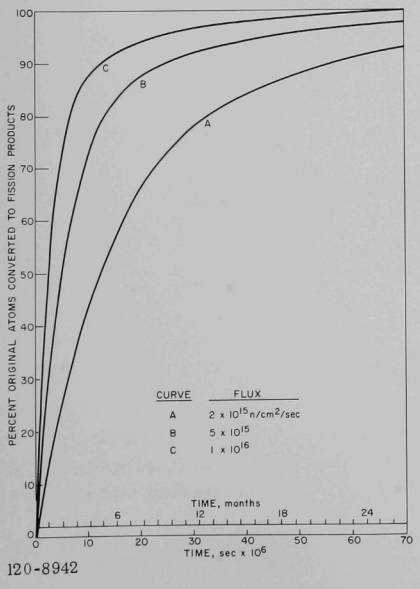

120-8942

Fig. 23

Percent Original Atoms Converted to Fission Products. Cm^{244} Target.

It will be seen in Figures 21-24 that an appallingly large amount of any of the targets eventually ends up as fission products rather than as the elements sought. From this point of view, controlled nuclear explosions as a source of very heavy elements have much appeal, since the desired elements are all formed essentially instantaneously. The high-loss stages, such as Cm^{245} fission, that are inevitable in a normal reactor irradiation are thus effectively bypassed.

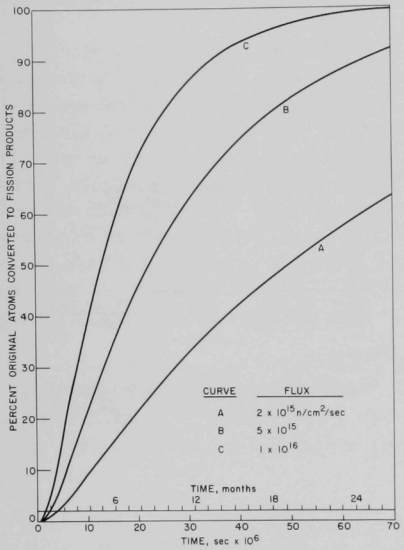

120-8943

Fig. 24

Percent Original Atoms Converted to Fission Products. Cf^{252} Target.

APPENDIX A

Calculation Methods for Tables 1 and 2

I. Definitions

$T_{1/2}$ = Half-life

λ = decay constant

σ_c = neutron capture cross section (thermal)

σ_F = fission cross section (thermal)

f = neutron flux ($n/cm^2/sec$)

ν = prompt neutrons emitted per fission

A = atomic number

M = atomic weight

Sp. Act. = Disintegrations per unit of time per unit of mass

II. Specific Activity (See Columns 4 and 5 of Table 1)

Sp. Act. (in same time units as $T_{1/2}$) = (λ)(atoms per unit weight) = $(0.693/T_{1/2})$(atoms per unit weight)

To obtain Sp. Act. as dis/sec/μg:

$$\text{Sp. Act.} = \left(\frac{0.693}{T_{1/2} \text{ in sec}}\right)\left(\frac{10^{-6} \times 6.02 \times 10^{23}}{A}\right) = \frac{\text{Constant}}{(T_{1/2})(A)}$$

The factor necessary to convert the quoted half-life to seconds can be included as part of the constant:

If $T_{1/2}$ is expressed in:	Constant is:
sec	4.16×10^{17}
min	6.95×10^{15}
hr	1.16×10^{14}
d	4.83×10^{12}
yr	1.32×10^{10}

Half-lives from column 2 were used to calculate specific activities given in column 4, and $T_{1/2}$ values from column 3 to calculate fissions/sec/μg for column 5.

III. Neutron Emission (See Column 6 of Table 1)

Asplund-Nilsson, Condé and Starfelt[12] have recently experimentally determined ν for the spontaneous fission of Cf^{252} to be 3.799 ± 0.034 neutrons/μg.

This value was assumed for all of the spontaneously fissioning nuclides considered in this report, and was used to multiply the figures of column 5 to obtain those in column 6.

IV. Cross Sections (See Columns 7, 8, and 9 of Table 1)

Values in columns 7 and 9 of Table 1 are quoted or estimated as described in the text. Column 8 data is derived from column 7 by the formula

$$cm^2/g = \frac{\sigma_c \times 10^{-24} \times 6.02 \times 10^{23}}{A} = \frac{0.602\sigma_c}{A}.$$

V. Helium Buildup (See Column 10 of Table 1)

The helium-buildup curves (see Figures 7-10) are cumulative, representing the integrated yield of alpha particles from the original target plus irradiation products. The data of column 10 are expressed as cc of helium produced per day per gram of nuclide, measured under standard conditions of temperature and pressure. These tabulated data are for rapid calculations; the curves are more exact, since all of the alphas emitted at a given time were summed and converted to milliliters of helium.

For alpha emitters:

$\frac{\text{Sp. Act.}}{6.02 \times 10^{23}}$ = moles helium produced per second per microgram;

$\left(\frac{\text{Sp. Act.}}{6.02 \times 10^{23}}\right)(8.64 \times 10^4)(10^6)$ = moles helium produced per day per gram = (1.44×10^{-13})(Sp. Act.);

$cc/day/gram = (\text{Sp. Act.})(1.44 \times 10^{-13})(22400) = (3.19 \times 10^{-9})(\text{Sp. Act.})$.

Since decay-scheme data are not available in most cases, the possibility of branching was ignored, and decay of alpha emitters was assumed to be 100% by that mode. Alphas from daughter nuclides or "feedback" chains were not considered, save in the case of Cf^{252} targets.

VI. Induced Fission (See Columns 2, 3, and 4 of Table 2)

N_B = number of atoms fissioned in time t = $N_A\sigma_F ft$;

N_A = atoms of target per microgram;

$$N_B = \frac{6.02 \times 10^{23}}{A \times 10^6} \times \sigma_F \times 10^{-24} \times f \times t;$$

$$\text{Fissions in one microgram per second} = \frac{6.02 \times 10^{-7}}{M_A} \times f \times \sigma_F.$$

VII. Heat from Fission (See Columns 5-8 of Table 2)

3×10^{10} fissions/sec = 1 W.

The values in columns 5, 6, and 7 were obtained by dividing the corresponding figures in columns 2, 3, and 4 by 3×10^{10}. Similarly, the values in column 8 were obtained by dividing the values of column 5 of Table 1 by the same quantity.

VIII. Heat from Nonfission Radioactive Decay (See Column 9 of Table 2)

Q values (average energy in MeV of particles emitted from the nuclide under consideration) were taken from the Table of Isotopes.[9] Where values were not given in that reference (for Cf^{255}, Fm^{257}, Fm^{259}, Mv^{259}, and Mv^{260}) a value of 7 MeV was assumed for alpha emitters, and a value of 1 MeV for beta emitters.

1 MeV/sec = 1.60×10^{-13} W

(Sp. Act.)(Q) = MeV/sec per μg of emitter

$W/\mu g = 1.60 \times 10^{-13} \times$ Sp. Act. $\times$ Q

IX. Percent of Original Atoms Converted to Fission Products

This quantity (see Figures 21-24) was calculated by summing the number of actinide element atoms (buildup products plus daughters) at any given time and subtracting from the original number of atoms present. The difference was assumed to be due to loss by fission. The expression of these data on a strict weight basis would, of course, involve corrections for mass and energy lost during the fission process as well as corrections for the mass and energy gained by target capture of pile neutrons.

REFERENCES

1. J. Milsted, P. R. Fields, and D. N. Metta, ANL-6756 (Aug 1963).

2. D. Metta, H. Diamond, R. F. Barnes, J. Milsted, J. Gray, Jr., D. J. Henderson, and C. M. Stevens, J. Inorg. Nucl. Chem., in press.

3. J. Milsted, P. R. Fields, and D. N. Metta, to be published.

4. E. K. Hulet, R. W. Hoff, H. R. Bowman, and M. C. Michel, Phys. Rev. 107, 1294-96 (1957).

5. D. C. Stewart, R. W. Anderson, and John Milsted, ANL-6933.

6. H. Bateman, Proc. Camb. Phil. Soc. 15, 423 (1910).

7. N. W. Isaac and J. W. Wilkins, ANL-6042 (Sept 1959).

8. E. K. Hyde, UCRL-9036, Rev. (April 1962).

9. D. Strominger, J. M. Hollander, and G. T. Seaborg, Revs. Mod. Phys. 30, 585-904 (1958).

10. S. Glasstone, Principles of Nuclear Engineering, D. Van Nostrand, Inc., New York (1955), p. 24.

11. R. E. Cote', R. F. Barnes, and H. Diamond, Phys. Rev. 134, 1281-84 (1964).

12. I. Asplund-Nilsson, H. Conde', and N. Starfelt, Nucl. Sci. Eng. 16, 124-30 (May 1963).